Journal Pre-proofs

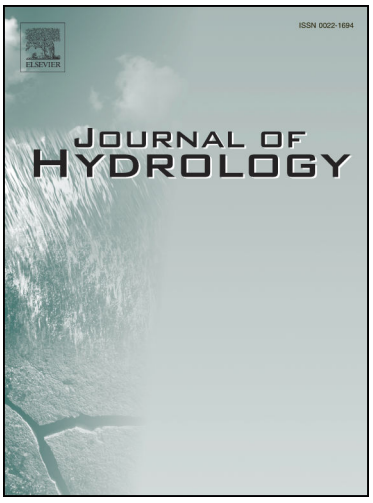

Research papers

2D Hydrodynamic approach supporting evaluations of hydrological response in small watersheds: implications for lag time estimation

Giuseppe Barbero, Pierfranco Costabile, Carmelina Costanzo, Domenico Ferraro, Gabriella Petaccia

PII: S0022-1694(22)00445-0
DOI: https://doi.org/10.1016/j.jhydrol.2022.127870
Reference: HYDROL 127870

To appear in: *Journal of Hydrology*

Received Date: 5 November 2021
Revised Date: 1 March 2022
Accepted Date: 20 April 2022

Please cite this article as: Barbero, G., Costabile, P., Costanzo, C., Ferraro, D., Petaccia, G., 2D Hydrodynamic approach supporting evaluations of hydrological response in small watersheds: implications for lag time estimation, *Journal of Hydrology* (2022), doi: https://doi.org/10.1016/j.jhydrol.2022.127870

2D Hydrodynamic approach supporting evaluations of hydrological response in small watersheds: implications for lag time estimation

Giuseppe Barbero[1], Pierfranco Costabile[2], Carmelina Costanzo[2], Domenico Ferraro[3],Gabriella Petaccia[1]

[1]*Department of Civil Engineering and Architecture, University of Pavia, 27100 Pavia, Italy.*

[2]*Department of Environmental Engineering, University of Calabria, 87036 Rende (Cosenza), Italy.*

[3]*Department of Civil Engineering, University of Calabria, 87036 Rende (Cosenza), Italy*

Corresponding author: Pierfranco Costabile (pierfranco.costabile@unical.it).

Keywords: *2D shallow water equations, integrated hydrodynamic-hydrologic models, distributed physically-based approach, hydrological response, lag time*

Abstract

The use of integrated flood models represents an approach of growing interest in the literature, being the hydrological and hydrodynamic flood processes described entirely within the two-dimensional (2D) hydrodynamic unsteady flow equations. Due to its ability in simulating complex spatial-temporal dependence of both the hydrodynamic and hydrologic responses of a catchment to rainfall events, this kind of approach paves the way to the development of novel lines of research in catchment hydrology. With particular reference to the lag time estimation, the paper focuses on three interrelated issues: 1) the use of the 2D-SWEs model to provide evidence on the variability of the lag time in small basins, 2) the description of the hydrologic response of small catchments based on characteristic times influencing the hydrodynamic response to rainfall events and 3) the representativeness of hydrodynamic-based rainfall-runoff scenarios in the description of the hydrologic response observed in real events. To that purpose, synthetic rainfall-runoff scenarios for different return periods are firstly generated to analyze the hydrologic response time in three ungauged basins. Then regressive formulas, based on *ad hoc* variables representing characteristic times, are introduced to interpret the variability shown by the computed lag time. Finally, the physical soundness of the proposed approach is tested against observed rainfall-runoff data in four additional basins. Despite all the simplifications introduced in the proposed approach, the regressive formulas provided a reasonably good agreement with the estimations of the lag time of the observed events, showing errors of the order of 30%. The comparison with the predictions of empirical literature formulas further confirms the potential of the proposed approach. This study represents the basis for future research on basin response to rainfall events through the use of a 2D integrated hydrodynamic-hydrologic modeling.

INTRODUCTION

Runoff processes at the catchment scale were analyzed extensively in the related literature (Beven, 2011). From the classical hydrological point of view, runoff is related to the precipitation input through several processes, finally resulting in a discharge hydrograph at the basin outlet. This approach is typically lumped or spatially semi-distributed, and often based on simplified or non-physical equations. In this context, the lumped unit hydrograph theory is one of the reference methods for rainfall-runoff computations (Clark 1945; Nash 1957; Rodriguez-Iturbe and Valdés, 1979; Kumar et al., 2007; Grimaldi et al., 2012; Rigon et al., 2016).

Precipitation surface runoff is characterized by extremely small water depths, and therefore it should be well-represented by the two-dimensional shallow water equations (2D-SWEs). 2D-SWEs models are not only able to compute runoff volume and outflow hydrographs, as provided by lumped models but, in addition, the spatial distribution of water depths as well as runoff velocities. Therefore, the results are not only physically-based, and thus arguably better, but also more complete, considering that more information is obtained (Caviedes-Voullième et al. 2012; Fernández-Pato et al., 2020).

Nowadays, the use of the 2D-SWEs approach as an integrated hydraulic-hydrologic model is more and more studied, since hydrological and hydrodynamic flood processes are not modeled in two different systems but entirely with the 2D hydrodynamic model. The use of this approach is a growing trend in rainfall-runoff applications, and several challenges can be identified in the literature: numerical methods to get stable and reliable results (Costabile et al., 2013; Cea and Bladé 2015; Xia et al, 2017; Yu and Duan, 2017), issues related to microtopography (Caviedes-Voullième et al. 2021), roughness (Kirstetter et al., 2016; Taccone et al., 2020), infiltration (Fernández-Pato et al., 2016; Ni et al., 2020), analysis of channels networks (Costabile et al., 2019, Costabile et al., 2022), computational speed up (Lacasta et al., 2015; Xia et al., 2016; Aureli et al., 2020; Morales-Hernández et al., 2021), generation of efficient numerical grids for reduction of computational times (Ferraro et al., 2020; Costabile and Costanzo, 2021), large scale flood modeling or real-time simulations (Ming et al., 2020; Bellos et al, 2020; Dullo et al., 2021).

Due to their ability in simulating complex spatial-temporal dependence of both the hydrodynamic and hydrologic responses of a catchment to a rainfall event (Caviedes-Voullième et al., 2021), this kind of approach paves the way to the development of further lines in catchment hydrology research. Specifically, an unexplored issue may be represented by how to exploit the hydrodynamic responses to a rainfall event, intrinsically provided by 2D SWEs simulations, for the evaluation of fundamental parameters that characterize the traditional hydrologic models and the hydrologic response to rainfall events. The catchment response is traditionally described in terms of time parameters providing information about the speed of response of a watershed to a storm event (Pavlovic and Moglen, 2008), such as time-to-peak, time of concentration, and lag time. These parameters are widely used as input to common hydrological design tools in the context of everyday engineering applications but, due to the several definitions (Talei and Chua, 2012) and estimations that can be found in the literature (Gericke and Smithers, 2014), resulting in very different design values, they remain ambiguous

and uncertain concepts of modern hydrology (Grimaldi et al., 2012; Michailidi et al., 2018; Beven 2020). In particular, the major inconsistency is represented by considering them as constant parameters of the basin rather than hydraulic variables, thus neglecting the role of flow velocities that may be particularly different if extreme or usual flood events are considered (Michailidi et al., 2018).

Flow velocities may be intrinsically related to the hydrodynamic response of a watershed and can be accurately described by a fully dynamic shallow water model. Therefore, it seems relevant to analyze what is traditionally seen as the hydrologic response in the light of the hydrodynamic response that can be now simulated by a sophisticated 2D SWE model running on high-resolution DEM.

More specifically, the original research questions posed in this paper are: can a 2D-SWEs model be used to provide evidence on the variability of the lag time in small basins? How to describe the hydrologic response of small catchments based on characteristic times influencing the hydrodynamic response to rainfall events? Can hydrodynamic-based rainfall-runoff scenarios be representative of the hydrologic response observed in real events? To the author's knowledge, no studies addressed these challenging issues which, therefore, represent the core and the focus of this study.

The paper is organized as follows. Section 2 aims at providing a literature framework related to the estimation of catchment response times, specifying some approaches that will be used in this work for comparative purposes. In Section 3, all the methodological issues are presented, highlighting the procedural steps implemented to realize to what extent the 2D hydrodynamic-based runoff modeling can support evaluations for the hydrologic response of a natural watershed. Section 4 shows the case studies analyzed in this work. Section 5 is devoted to the results whereas the limitations and impacts of this study are discussed in Section 6. Finally, the most significant conclusions of this work are summarized in section 7.

2. BACKGROUND

Two of the most widely used definitions of the lag time are (1) time to centroid: time interval between the centroid of the effective rainfall and the centroid of direct runoff, and (2) time to peak: time interval between the centroid of effective rainfall and peak of direct runoff (see, for example, Snyder 1938). Referring to the time to peak definition, a plethora of empirical formulas exist (Hickok et al., 1959; Watt and Chow 1985; NERC, 1975; Mimikou 1984; Loukas and Quick, 1996; Yu et al., 2000; Folmar and Miller, 2008; Haaktanir &Sezen 1990; McEnroe and Zhao, 2001; NRCS, 2010; Gericke and Smithers, 2014). Similarly, several studies are based on the definition of lag time as the time to centroid, which is considered also in this paper. In this context, the lag time is sometimes related to the catchment area *A* (Mitchell, 1948; Boyd, 1978; Ermini and Fiorentino, 1989; Corradini et al., 1995, Melone et al. 2002). Some authors proposed simplified

formulas in which the lag time is related to basin characteristics, like the ratio L/S being L the basin length and S the basin slope or adding A, the imperviousness factor i_p, and the basin Curve Number (CN) (Nash, 1960; Amorocho and Brandstetter, 1971; Putnam, 1972; Rossi, 1974; Haaktanir and Sezen, 1980; Leopold, 1991; Simas and Hawkins, 2002). Other studies provided estimations of the lag time considering also the influence of rainfall (Askew, 1970, Boyd et al., 1979; Selvalingam et al., 1987; Boyd and Bufill, 1989, Delleur and Rao, 29174, Wu et al., 2016). These papers may be considered as a part of a more general research field that overcomes the concept of constant response times, in a basin (Pavlovic and Moglen, 2008; Grimaldi et al., 2012; Meyersohn, 2016). Several formulas mentioned above will be used later on in this work for comparative purposes (see section 3.3).

3. METHODOLOGICAL ISSUES

To face the challenging research questions posed in the introduction, the methodology proposed in this work is based on the flow chart presented in Figure 1. The first step is the generation, for three ungauged basins (see section 4.1), of rainfall-runoff scenarios for different return periods to be used for the estimation of the lag time. The purpose of this step is to evaluate the role of 2D-SWEs modeling for providing evidence on the variability of the lag time in small basins. The lag time definition used in this work is the time to the centroid (see section 2).

The second step aims at introducing formulas based on characteristic times somehow related to the hydrodynamic response to rainfall events, able to interpret the behavior observed by the lag time in a specific basin.

The goal of the final step is to understand to what extent the lag time computed using the regressive formulas, calibrated for a few ungauged basins and based on numerical rainfall-runoff scenarios, can be considered as representative of the hydrologic response observed in real events. To that purpose, the performances of the regressive formulas derived before will firstly be compared to the observed lag time estimations, and then discussed in the light of the variability of the predictions based on the applications of several empirical formulas mentioned in section 2.

[Figure 1 Approximately here]

3.1 Generation rainfall-runoff scenarios

The method used for the generation of rainfall-runoff scenarios is represented by the flowchart in Figure 2. Synthetic storm events were generated considering six rainfall events, associated to a return period T equal to 5, 10, 30, 50, 100 and 200 years respectively. The rainfall intensity-duration curve was taken from the Regional Agency for the Protection of the Environment (ARPA) website, considering data from 1987 to 2011 (http://idro.arpalombardia.it). The temporal distribution of the rainfall event was evaluated using the Chicago hyetograph. To add some variability in the distribution of the rainfall volume, three different choices were made for the temporal position of the peak value (CH), variable in the range [0.3-0.7] times the overall duration of the event. This choice is motivated in part by analyses of observed events

related to the geographical areas considered in this work, for which the previous range is able to represent more than 70% of the cases, being CH=0.5 the most frequent situation. On the other hand, some works on this field (Keifer and Chu, 1957; Arnell, 1983) highlighted CH values between [0.3-0.5] as very common worldwide.

Net-rains were estimated using the original Soil Conservation Service (now NRCS) Curve Number (SCS-CN) method (SCS 1985). This approach is based on just one-parameter (CN), widely adopted, discussed and refined (see for example, Ponce and Hawkins 1996; Bhuyan et al., 2003) even in the more recent literature (Shi et al., 2021).

[Figure 2 Approximately here]

As for the CN II estimation, we assumed a uniform value in the basins. In particular, the distribution of the CN II throughout the watersheds was firstly obtained using both the lithologic property maps and the land use maps, provided by the Corine Land Cover, on the basis on the well-known SCS-CN approach (SCS 1985). Then the spatial weighted average value, on the basis of the area covered by each class, was computed in order to provide estimation of the net rainfall. The CN II values were found equal to 84, 88 and 89 for the Ardivestra, Versa and Scuropasso, respectively. Considering the scenario-based approach used in this work, AMC (Antecedent Moisture Conditions) levels were arbitrarily assumed in such a way to cover a wide range of cases. Therefore, CN III and the CN I values were also computed. Hence, the synthetic gross rainfall events related to the six return times were manipulated using the SCS-CN approach, assuming all the three options for the AMC levels and three different peak positions leading to a total of 30 simulations for each catchment.

The synthetic net rainfalls generated as described above were used to initialize the 2D SWEs model developed by the authors. This model is considered appropriate for the purposes of this work since it provided reliable results in both fluvial flood inundation mapping in urban environments (Costabile et al., 2020; 2021a; Padulano et al., 2021) and runoff simulations at basin scale (Costabile et al., 2019; Costabile et al., 2021b), in which the rainfall is directly applied to the computational grid as the applications shown in this work. The 2D SWEs model required the estimation of the Manning roughness coefficients. A non-uniform distribution of the roughness coefficients was assumed, in which the Manning coefficients were derived according to Chow (1959) on the basis of the homogeneous land use map, provided by the Corine Land Cover, as usually performed in 1D and 2D computations (see for example Costabile et al., 2015). To provide a rough idea of the computed values, the spatial weighted Manning value, for each basin, is reported in table 2. As an example, the Land Cover and geological maps used for the generation of the spatial distribution of the CN II for the Ardivetsra basin are shown in figure 3.

[Figure 3 Approximately here]

3.2 Characteristic times for interpreting the variability of the lag time observed from hydrodynamic computations

Two approaches are followed here. The first one is based on a conceptual model whereas the second one is essentially empiric.

3.2.1 *Conceptual approach*

The conceptual approach takes advantage of the kinematic wave theory. As it is known, analytical equations representing the lag time or time to concentration can be obtained considering a uniform rainfall R along an impervious plane with a uniform slope S_0 and length L_0, assuming a duration such that steady-state conditions are reached (rainfall rate equal to runoff rate per unit area). Under these hypotheses, the travel time from a generic point x on the slope to the outlet of the plane ($x=L_0$) can be defined as:

$$T_x = \int_x^{L_0} \frac{dx}{V_x} \tag{1}$$

where V_x is the flow velocity. The lag time $T_{Lag,K}$ can be defined as the average time of travel along the plane and, therefore, can be computed as:

$$T_{Lag,K} = \frac{1}{L_0}\int_0^{L_0} T_x dx = \frac{5}{8}\left(\frac{nL_0}{\sqrt{S_0}}\right)^{0.6} R^{-0.4} \tag{2}$$

where n indicates the Manning coefficient. Equation (2) can be obtained by coupling the mass continuity equation and the Manning equation (Yu et al., 2000). Following the same theory, it is also possible to obtain the time of concentration $T_{con,K}$ as:

$$T_{con,K} = \left(\frac{nL_0}{\sqrt{S_0}}\right)^{0.6} R^{-0.4} \tag{3}$$

which corresponds to the time at which the plane is in equilibrium or, in other words, to the travel time to the downstream end of the plane (Singh, 1997; Zuazo et al., 2014). Being related to the same theory, equations (2) and (3) can be used indifferently. However, some specifications should be introduced in practice, considering that no planes but natural watersheds are considered. In particular, the total length L_0 is assumed equal to the length of the main river course L, S_0 is set equal to the mean slope of the basin S, and R is set equal to the mean net rainfall intensity I_m. Finally, a synthetic value of the Manning coefficient is assumed, evaluated as spatial weighted average on the basins of the homogeneous land cover areas. Therefore, the regression laws discussed in section 5.2 will be based on the values reported in Table 2. To consider the variability of the rainfall intensity, the multiplier M shown in equation (4) is also considered:

$$M = \left(\frac{I_m}{I_{\max}} \right)^{\alpha} \tag{4}$$

being I_{max} the maximum net rainfall rate and α a parameter to calibrate. Basically, two variables are considered hereafter:

$$X_1 = \left(\frac{nL}{\sqrt{S}} \right)^{0.6} I_m^{-0.4} \tag{5}$$

$$X_2 = M \left(\frac{nL}{\sqrt{S}} \right)^{0.6} I_m^{-0.4} \tag{6}$$

that may be seen as characteristic times potentially influencing the hydrodynamic response of watershed to a rain event.

3.2.2 *Empirical approach*

Attention was devoted to finding relations having the structure of equation (7), where relevant variables that may influence the hydrodynamic response of the watershed are considered together:

$$T_{Lag} = F(n, A, L, L_t, S, I_m, I_{\max}) \tag{7}$$

in which L_t is the total length of the channel network. By manipulating these parameters, characteristic times of the watershed can be obtained, easy to estimate using a common GIS tool. For example, three characteristic times, reported in equations (8) can be introduced:

$$\theta_1 = \frac{L}{I_{\max}};\ \theta_2 = \frac{n}{S}\left(\frac{A}{L} \right)^{1/3};\ \theta_3 = \frac{n}{S}\left(\frac{A}{L_t} \right)^{1/3} = \frac{n}{S} D^{-1/3} \tag{8}$$

where D represents the drainage density, defined as the ratio between L_t and A. The first characteristic time, θ_1, takes into account topographic (L) and rainfall data (I_m) whereas the second and third ones, θ_2 and θ_3, consider hydraulic (n) and topographic/network-based information (A, D, L, S). It should be observed that θ_2 and θ_3 are very similar except for the characteristic length assumed to obtain the characteristic time.

Starting from equation (8), the two variables described by equation 9 will be considered in the paper:

$$X_3 = (\theta_1 \theta_2)^{0.5}, X_4 = (\theta_1 \theta_3)^{0.5} \tag{9}$$

3.3 Soundness of the overall approach: comparison with observed data and predictions from literature formulae

The reasoning followed for this part is depicted in Figure 4. Specifically, we selected four basins (see section 4), different from the ones used for the generation of rainfall-runoff scenarios, where rainfall-runoff data were available for the estimation of the lag time of the events. To take into account some uncertainty in the estimation of the lag time of the selected events, a range of plausible values were considered, so that two different estimations were provided. In the first estimation, the net-rainfall was obtained from the gross one using the SCS-CN method, in which the CN value is considered as a calibration parameter. Then the time interval between the centroid of the effective rainfall and the centroid of the direct runoff is computed. The direct runoff is computed eliminating from the observed discharge the base flow. In the second approach, lag time is evaluated as the interval between the centroid of the effective rainfall evaluated with the SCS-CN method, as before, and the centroid of the discharge hydrograph computed using a hydrological model.

Among the different hydrological methods available for the rainfall-runoff modeling, the authors chose the Clark method (Clark, 1945) which is frequently used in the literature (see e.g. Kazezyılmaz-Alhan et al 2021, Ghorbani et al. 2019).

Both the estimations were carried using the well-known software HEC-HMS, developed by the U.S. Army Corps of Engineers (Fieldman 2000), which is one of the most widely used hydrological software in the engineering practice (see for example Laouacheria and Mansouri, 2015).

[Figure 4 Approximately here]

These two reasonable estimations of the lag time will provide a range of values, $[T_{Lag,inf}, T_{Lag,sup}]$, to be used as a reference. Specifically, for each observed event, the error E made by a specific regression equation is computed as:

$$E = \begin{cases} 0, & \text{if } T_{Lag,P} \in \left[T_{Lag,\inf}, T_{Lag,\sup}\right] \\ \dfrac{\left|T_{Lag,P} - T_{Lag,R}\right|}{T_{Lag,R}}, \; T_{Lag,R} = \min\left(\left|T_{Lag,P} - T_{Lag,\inf}\right|, \left|T_{Lag,P} - T_{Lag,\sup}\right|\right) & \text{, if } T_{Lag,P} \notin \left[T_{Lag,\inf}, T_{Lag,\sup}\right] \end{cases} \quad (10)$$

in which $T_{Lag,P}$ is the lag time value predicted by the proposed regression equations and $T_{Lag,R}$ is the extreme point of the estimated lag time target range closer to $T_{Lag,P}$. In other words, no error is made if the predicted value falls within the target range otherwise the absolute percentage error is computed in respect to the extreme point of the interval closer to $T_{Lag,P.}$

The error provided using the proposed formulae will be not only analyzed to realize how far the predictions are from the target range, but also in comparison to the values given by the application of literature formulas that use the same definition of the lag time considered here (time to centroid). In particular, we used three groups of formulas: the first one is mainly dependent on the basin area, the second one uses other topographic characteristics whereas the third one considers also the dependence from rainfall characteristics (see Table 1).

[Table 1 Approximately here]

The symbols used in Table 1 have been defined before except from L_{CA}, distance between the centroid and the estuary (km), P_E, the effective rainfall (mm), and D_{PE}, duration of effective rainfall (h). In all the formulas, A and L are expressed, respectively, in (km^2) and (km) whereas the rainfall intensity are in (mm/h).

4. CASE STUDIES AND AVAILABLE DATA

Six Italian basins were considered in this study. Three basins were used for the generation of rainfall-runoff scenarios (Figure 5). Specifically, the Ardivestra basin is located in the central Oltrepo Pavese (Figure 5b) whereas the Versa basin (Figure 5c), and Scuropasso basin (Figure 5d) are located in the north-eastern part of the Oltrepò Pavese. All of them are part of the Po River basin. A high-resolution airborne LiDAR covers the three catchment areas, providing a sampling density of four points over 1 m^2.

[Figure 5 Approximately here]

Furthermore, four additional basins were used to validate the methodology by using registered rainfall-runoff events (Figure 6). The Bevera (Figure 6b) and Lambro basin (Figure 6c), are tributaries of the Po River, located in the pre-alpine area, in Lombardy Region. Figure 6(d) shows the Turbolo catchment, a tributary of the Crati River whereas Figure 6(e) shows the Ancinale mountainside sub-catchment of the homonymous reach, both located in the Calabria region (South of Italy). For all these catchments, 5m resolution DEMs were used.

The main characteristics of all the basins are detailed in Table 2, in which all the symbols have been defined before except from z_{max}, z_{mean} and z_{min} that are the maximum, average and minimum elevations respectively. All these data were derived in Quantum GIS 3.14 using a high-resolution Digital Terrain Model (DTM) and Corine land cover geo-referenced database.

[Figure 6 Approximately here]

[Table 2 Approximately here]

The observed rainfall-runoff data considered for validation purposes are shown in Figure 7, available on the official web site of regional agencies for the protection of the environment (*ARPA Lombardia and ARPA Calabria - Centro Regionale Multi Rischi*). The authors intentionally chose very different events in terms of duration, rainfall intensity, and peak discharge to test the overall approach using complex and highly variable situations. These events are considered to be representative of the rainfall-runoff process characterizing these watersheds.

[Figure 7 Approximately here]

5. RESULTS

5.1 Numerical evidence of the variability of the lag time using the rainfall-runoff scenarios

Following the methodology proposed in section 3.1 (see also Figure 2), the results related to the Scuropasso basin are shown in figure 8.

[Figure 8 Approximately here]

Figure 8a and Figure 8b show the influence of the return period in the lag time computations according to the antecedent soil moisture conditions analyzed and the peak position, respectively. The computed lag times show a significant variability for a given basin, at least for the lower return periods. This consideration holds regardless of both the initial soil moisture condition and the peak position (Figures 8a,b). Indeed, a greater variability is associated to lower return periods whereas seems to be limited for the higher ones, confirming some indication in the literature based on the assumption that for high-magnitude storm events the lag time dependence from rainfall characteristics is negligible (Di Lazzaro 2009). Globally, lag time value seems to depend not only on the geomorphological features of the watershed but also on the characteristics of the effective rainfall event, which, in turn, is related to the considered return period. Figures 9a and Figure 9b seem to suggest a very good best fit power-law relation between the lag time and the return period. This result is further confirmed by the analysis of Figure 9c, which explicitly shows the influence of the mean rainfall intensity on the lag time value for the three considered catchments. Specifically, the computed lag time decreases as the mean rain intensity increases. Also, in this case, a power-law relation seems to interpret very well the data, since the coefficients of regression R^2 range between 0.83 and 0.93. It may be significant to highlight that the exponents of the power law relations range between 0.35 and 0.52.

[Figure 9 Approximately here]

5.2 Interpretation of the variability of the observed lag time

Figure 10 shows strong correlations between the lag time and all the four variables, as synthetically represented by the coefficient of determination R^2 reported in table 3. As for the variable X_2, the value of α=0.3 (see equation 4) provided the best results. The power-law reveals to be a proper best-fit formula, even though the regression equations related to X_1 and X_2 are substantially linear. The formulas shown in table 3 allow the estimation of the lag time in (h) for L and L_t in (m), D in (m^{-1}), A in (m^2) and rainfall intensities in (m/s).

[Figure 10 Approximately here]

[Table3 Approximately here]

5.3 Comparison with observed data and literature formulas

The predictive results obtained using the four formulas shown in table 3 were evaluated against observed data on the four basins described in section 4.2. Specifically, a reasonable evaluation of the lag time for the 14 selected events was carried out, computing the target range as described in Figure 4. The parameters of the Clark method, implemented in HEC-HMS, were calibrated so that a good agreement between the observations and simulated discharges was obtained. In particular, the Nash-Sutcliffe model efficiency coefficient (Nash and Sutcliffe 1970) for the HEC-HMS simulations ranges between 0.88 and 0.99, confirming a very good fit with the real events. As an example, the comparison between simulated and observed discharges for three events is shown in Figure 11. It may be of interest to underline that, according to the simulations performed in HEC-HMS, the events are characterized by net rains having the following features: 1) the mean and maximum values ranges are, respectively, [0.7-10] mm/h and [3-67] mm/h; 2) the duration range is [2-42] h; 3) the cumulative values range is [15-51] mm/h.

[Figure 11 Approximately here]

The estimated lag time target range provided by the HEC-HMS software for each event is shown in blue and red in Figure 12, from which one can deduce its variability for different events within a specific basin. The estimated lag time values show a significant variability (56.1%, 60.1%, and 110% for the Bevera, for the Lambro, and the Ancinale Basin respectively). Figure 12 shows also the lag time values obtained with the 4 proposed regressions, which vary accordingly, even though that variability is not always represented by the proposed regressions. This might be explained by a combination of two factors: 1) the simplified assumptions introduced to generate the synthetic rainfall-runoff scenarios, not always representative of what occurs for natural events and 2) lack of relevant information in the variables X_1, X_2, X_3, and X_4 introduced to interpret the variability of the lag time.

Significant variability is found within the results obtained using the proposed regression laws, even though the mean value of the errors seems to be comparable. Except for equation T_L-X_1, which seems to provide slightly larger variations, the mean value of the errors is approximately 30% (see table 4). Equation T_L-X_4 provided the best prediction in most cases. The overall results obtained using the regression formulas seem to be very promising, though they have been calibrated using synthetic rainfall-runoff simulations in very few basins.

[Figure 12 Approximately here]

[Table 4 Approximately here]

The physical soundness of the proposed approach can be further appreciated when comparing the predictions of empirical formulas proposed in the literature. Specifically, all the formulas reported in table 1 were applied, but the results obtained using F12 were not considered in the following analyses because they are too far from the observed ones.

Great variability was found among the predictions, as reported in the box plot of Figure 13. When compared to the lag time target range, a very large variability is found in the literature formulas, as reported in table 5, in which the best and the second-worst results (the first one is excluded *a priori*) are highlighted in green and red respectively. An average error of 45%, is obtained if the worst predictions are neglected, whereas 55% is found if all the data are considered. These values are greater than the ones derived from the proposed regressions.

[Figure 13 Approximately here]

[Table 5 Approximately here]

5. DISCUSSION: limitations of the work, potential impacts of the research and future works

Concerning the modeling approach, one of the major limitations of this work is represented by the simplification introduced in the description of the hydrological processes for surface runoff generation. This paper only considers the infiltration excess runoff, setting the net rainfall computed using the SCS-CN method as input of the SWEs model. A more physically-based approach would be represented by the computation of the infiltration losses directly in the SWEs model (see for example Bout and Jetten, 2018; Ming et al., 2020; Ni et al., 2020; Bellos et al, 2020), even though this would have added further uncertainty due to the estimation of soil parameters regulating this process (Tügel et al., 2021). A second limitation is represented by the reduced number of watersheds used, if compared to the recent studies dealing with the estimation of the hydrologic response's times in natural watershed (see for example Ravazzani et al., 2019; Langridge et al., 2020). Furthermore, this study does not account for the spatial variability of rainfall, which is expected to affect catchment-scale hydrological response and the accuracy of predictions (see for example Pechlivanidis et al., 2017; Zheng et al., 2018). It should be also recalled that only the definition of time-to-centroid, for the lag time estimation, has been considered in this work. Further studies, that cannot find room here, are required to understand the soundness of the methodology developed in this work considering other definition of the lag time, as time to peak.

Despite all these limitations, it seems important to underline that the relations introduced here for lag time estimation are very encouraging. Though calibrated for a few ungauged basins and based on numerical rainfall-runoff scenarios, the predicted lag time is in reasonably good agreement with the observed ones. Furthermore, the comparison between those relations and the experimental equations proposed in the literature further highlights the physical soundness of the proposed approach, since the average error of the proposed regressions is even lower than the mean value of the literature ones. Finally, the findings of this research provide further evidence about the variability of the lag time, at least in small basins, confirming the results of the previous studies on this (see section 2). It may be of interest to underline that the mean value of the scale exponents of the power-law relations, between the lag time and the mean rainfall intensity only, observed from the rainfall-runoff scenarios in the three ungauged basins (Figure 8c), is about 0.45 that agrees with the

experimental observation provided by Zhang et al. (2007). Moreover, the combination of the proposed characteristic times influencing the hydrodynamic response to rainfall, which considers geomorphological, network-based, hydraulic, and rainfall information, seems to be a promising way to interpret that variability. It seems important to observe that the drainage density *D* is rarely used in the literature to analyze the time response of the watershed (the work by Langbein (1947) is an exception). In particular, *D* seems to play a significant role, confirming what was observed in other recent studies (Amiri et al., 2019). Therefore, it can be considered in the future in those lines of research focused on the effects of geomorphological parameters for the lag time estimations and flood hazard assessment (see for example Gericke, 2019; Bhat et al., 2019).

7. CONCLUSIONS

This paper focuses on the analysis of the traditional hydrologic response times in the light of the hydrodynamic response simulated by an integrated 2D SWEs modeling running on high-resolution DEM. Therefore, the novelty introduced in this work has been represented by the use of a physically-based approach for the analysis of the variability of the watershed response time, which is traditionally considered as a constant parameter to be evaluated using morphological values. In particular, attention was devoted to the analysis of the lag time defined as time-to-centroid.

The main findings of this research are listed below.

1) The results of numerical investigations based on a rainfall-runoff scenarios on three small basins, highlighted that the lag time cannot be considered as a constant parameter of the catchment. In particular, a clear influence of the return period in the lag time estimations was observed, meaning that the characteristics of the rainfall events are among the main variables influencing the lag time;
2) the variability of hydrologic response time observed in the numerical rainfall-runoff scenarios was described by a combination of characteristic times influencing the hydrodynamic response of a basin to rainfall events. Specifically, four formulas have been introduced, that proved to be able to predict the lag time variability observed for three small ungauged basins;
3) the regressive formulas provided results in a reasonably good agreement with the estimations of the lag time related to the observed events, showing errors of the order of 30%. Their performances have been further highlighted in the light of the variability of the predictions based on the applications of several empirical literature formulas, proving to be very competitive and encouraging. Therefore, they may be considered as representative of the hydrologic response observed in real events.

Finally, it should be stressed that more advanced modeling of the hydrological processes within the 2D SWEs may further improve the results presented in this work. Therefore, attention should be focused not so much on the regressive formulas presented here but on the overall approach, which may represent the basis for future research on basins response to rainfall events through the use of integrated hydrodynamic-hydrologic modeling.

TABLES

ID Formula	Equation	Reference	Group
F1	$1.193 \cdot A^{0.33}$	Corradini et al. (1995)	1
F2	$2.51 \cdot A^{0.38}$	Boyd (1978)	1
F3	$0.344 \cdot A^{0.5}$	Ermini & Fiorentino (1989)	1
F4	$0.5392 \cdot A^{0.6}$	Mitchell (1948)	1
F9	$\frac{0.493}{\left(1+i_p\right)^{1.433}} \cdot A^{0.512}$	Delleur & Rao (1974)	1
F5	$0.295 \cdot \left(\frac{L}{\sqrt{S}}\right)^{0.77}$	Rossi (1974)	2
F6	$1.02 \cdot \frac{L^{0.3}}{S^{0.33}}$	Nash (1960)	2
F7	$0.2685 \cdot L^{0.841}$	Haaktanir & Sezen (1980)	2
F8	$\frac{0.2263}{S^{0.1505}} \cdot \left(\frac{A}{L}\right)^{0.5937} \cdot \left(\frac{25400}{\text{CN-254}}\right)^{0.3131}$	Simas & Hawkins (2002)	2
F10	$\frac{0.082}{i_p^{0.57}} \cdot \left(\frac{L}{\sqrt{S}}\right)^{0.5}$	Putnam (1972)	2
F11	$1.274 \cdot \frac{A^{0.458} \cdot D_{PE}^{0.371}}{P_E^{0.267} \cdot \left(1+i_p\right)^{1.662}}$	Delleur & Rao (1974)	3
F12	$1.53 \cdot 10^{-9} \frac{A^{0.959} \cdot L_{CA}^{0.029} \cdot P_E^{0.122}}{n^{4.5} \cdot L^{1.46} \cdot S^{2.09} \cdot i_{\max}^{0.191}}$	Wu et al. (2016)	3

Table 1 – Literature formulas considered for comparative purposes, grouped on the basis of the parameters used for the estimation of the lag time: equations mainly characterized by basin area (Group 1), other topographic features (Group 2) and also influenced by rainfall data (Group 3)

	Ardivestra	Versa	Scuropasso	Bevera	Lambro	Turbolo	Ancinale
A (km^2)	47.32	55.38	36.84	25.57	54.06	29.10	45.45
L (km)	24.09	23.62	18.27	13.26	15.50	13.68	11.62
L_t (km)	198.38	265.44	163.57	66.48	92.23	64.02	110.97
S	0.32	0.19	0.22	0.22	0.47	0.31	0.24
z_{max} (m a.s.l)	797.18	665.92	532.61	890	1452.56	1002.66	1398.29
z_{mean} (m a.s.l)	421.99	26.20	259.61	425.02	766.85	320.49	946.47
z_{min} (m a.s.l)	190.97	71.31	84.87	261.43	326.27	80.74	746.47
D (km^{-1})	4.2	4.8	4.4	2.6	1.8	2.2	2.2
n (sm$^{-1/3}$)	0.05	0.055	0.055	0.06	0.062	0.043	0.097
i_p (%)	0.25	0.68	1.68	20.67	11.46	4.92	5.85
L_{CA} (km)	11.35	9.57	11.27	7.41	6.74	7.56	7.12

Table 2: Main features of the catchments considered in this work

Variable	Regression law	R^2	Equation ID
X_1 (h)	$T_{LAG} = 0.369 \cdot X_1^{1.02}$	0.87	T_L-X_1
X_2 (h)	$T_{LAG} = 0.605 \cdot X_2^{1.07}$	0.90	T_L-X_2
X_3 (h)	$T_{LAG} = 1.84 \cdot X_3^{0.82}$	0.88	T_L-X_3
X_4 (h)	$T_{LAG} = 0.23 \cdot X_4^{0.85}$	0.86	T_L-X_4

Table 3. Regression laws for the estimation of the lag time as a function of the variables introduced in this work

	T_L-X_1	T_L-X_2	T_L-X_3	T_L-X_4
B1	0.43	0.26	0.17	0
B2	0.50	0.52	0.49	0.43
B3	0.43	0.42	0.39	0.31
B4	0.39	0.34	0.29	0.21
B5	0.58	0.51	0.46	0.39
L1	0.62	0.10	0	0.06
L2	0.18	0.22	0.20	0.15
L3	0.62	0.64	0.63	0.61
L4	0.40	0.39	0.37	0.33
A1	0	0	0	0
A2	0.54	0.57	0.63	0.73
A3	0.26	0.34	0.33	0.30
A4	0.09	0.13	0.25	0.33
T1	0.21	0	0.19	0.34
Mean (Bevera)	0.47	0.41	0.36	0.27
Mean (Lambro)	0.46	0.34	0.30	0.29
Mean (Ancinale)	0.22	0.26	0.30	0.34
Mean (overall)	0.37	0.32	0.31	0.30

Table 4. Absolute errors made by the proposed regressions in respect to the Lag Time target range (the best and the worst results are highlighted in green and red respectively).

	F-1	F-2	F-3	F-4	F-5	F-6	F-7	F-8	F-9	F-10	F-11	
L1	0.39	0.52	0.70	**0.28**	0.64	0.36	0.59	**0.75**	0.66	0.81	0.11	
L2	0.32	0.60	0.66	**0.19**	0.60	0.29	0.54	**0.71**	0.61	0.79	0.21	
L3	0.35	0.55	0.67	**0.22**	0.61	0.31	0.56	0.73	0.63	0.80	**0.06**	
L4	0.16	0.89	0.58	**0**	0.5	0.12	0.43	0.65	0.52	**0.74**	0.0	
B1	0.38	0.49	0.69	**0.26**	0.63	0.35	0.58	**0.74**	0.65	0.81	0.35	
B2	0.85	3.74	**0.05**	**1.70**	0.15	0.23	0.12	0.16	0.35	0.41	3.07	
B3	0.83	3.70	**0.04**	**1.67**	0.21	0.22	0.11	0.15	0.34	0.45	1.35	
B4	0.23	2.16	0.29	**0.80**	0.46	0.17	0.25	0.22	**0.09**	0.63	0.09	
B5	0.34	2.43	0.21	**0.95**	0.40	0.07	0.16	0.13	**0**	0.58	0.79	
A1	**0**	1.12	0.38	0.16	0.48	0.09	0.44	0.30	0.14	0.46	**0.85**	
A2	0.21	2.1	0.18	0.70	0.30	**0**	0.25	0.89	**0**	0.28	**1.89**	
A3	0.20	0.80	0.56	**0**	**0.63**	0.35	0.6	0.1	0.39	0.62	0.50	
A4	0.15	0.98	0.53	**0.1**	0.61	0.31	0.58	0.21	0.35	0.60	**0.85**	
T1	0.41	2.50	0.13	**0.74**	0.07	0.28	**0**	0.01	0.01	**0**	1.15	
Mean (Lambro)	0.56	3.00	**0.15**	**1.28**	0.30	0.17	0.16	0.16	0.20	0.52	1.32	0.48 (0.71)
Mean (Bevera)	0.32	0.58	0.66	0.19	0.60	0.29	0.54	**0.72**	0.61	0.79	**0.15**	0.47 (0.50)
Mean (Ancinale)	**0.14**	1.25	0.41	0.23	0.50	0.19	0.47	0.37	0.22	0.49	**1.02**	0.48 (0.40)
Mean (overall)	0.35	1.6	0.41	0.55	0.45	**0.23**	0.37	0.41	0.34	0.57	**0.80**	**0.45** (0.55)

Table 5. Absolute errors made by the literature formulas in respect to the Lag Time target range. The number in brackets refers to the mean value computed using all the values, without neglecting the worst result

ACKNOWLEDGMENTS

The authors would like to thank Prof. Ugo Moisello for both his critical reading of the manuscript and all his fruitful comments and suggestions.

REFERENCES

Amiri, B.J., Gao, J., Fohrer, N., Adamowski, J., Huang, J., 2019. Examining lag time using the landscape, pedoscape and lithoscape metrics of catchments. Ecological Indicators, 105, pp. 36-46.

Amorocho, J., Brandstetter, A., 1971. Department o] Water Science and Engineering, University of California. Water Resour. Res. 7, 1087–1101.

Arnell, V., Harremoes, P., Jensen, M., Johansen, N.B., Niemczynowicz, J., 1983. Review of rainfall data and application for design analysis. Water Science and Technology, 16 (8/9), 1:45.

Askew, J W, 1970. Derivation of Formulae for Variable Lag time. J. Hydrol. 10, 225–242.

Aureli, F., Prost, F., Vacondio, R., Dazzi, S., Ferrari, A.,2020. A GPU-accelerated shallow-water scheme for surface runoff simulations. Water (Switzerland), 12 (3), art. no. 637.

Bellos, V., Papageorgaki, I., Kourtis, I., Vangelis, H., Kalogiros, I., Tsakiris, G., 2020. Reconstruction of a flash flood event using a 2D hydrodynamic model under spatial and temporal variability of storm. Natural Hazards, 101 (3), pp. 711-726.

Bhat, M.S., Alam, A., Ahmad, S., Farooq, H., Ahmad, B., 2019. Flood hazard assessment of upper Jhelum basin using morphometric parameters Environmental Earth Sciences, 78 (2), art. no. 54.

Bhuyan, S.J., Mankin, K.R., Koelliker, J.K., 2003. Watershed - Scale AMC selection for hydrologic modeling. Transactions of the American Society of Agricultural Engineers, 46 (2), pp. 303-310.

Beven, K., 2011. Rainfall-runoff modelling: the primer. John Wiley&Sons.

Beven, K., 2020. A history of the concept of time of concentration. Hydrol. Earth Syst. Sci. 24, 2655–2670.

Bout, v. B., Jetten, V. G., 2018. The validity of flow approximations when simulating catchment-integrated flash floods. Journal of Hydrology, 556, 674–688.

Boyd, M.J., 1978. A storage-routing model relating drainage basin hydrology and geomorphology. Water Resour. Res. 14, 921–928.

Boyd, M. J., Bufill, M. C., 1989. Determining runoff routing model parameters without rainfall data. Journal of Hydrology, 108, 281-294.

Boyd, M. J., Pilgrim, D. H., Cordery, I., 1979. A storage routing model based on catchment geomorphology. Journal of Hydrology, 42(3-4), 209-230.

Caviedes-Voullième, D., Ahmadinia, E., Hinz, C., 2021. Interactions of Microtopography, Slope and Infiltration Cause Complex Rainfall-Runoff Behavior at the Hillslope Scale for Single Rainfall Events. Water Resources Research, 57 (7), art. no. e2020WR028127, .

Caviedes-Voullième, D., Garcìa-Navarro, P., Murillo, J., 2012. Influence of mesh structure on 2D full shallow water equations and SCS curve number simulation of rainfall/runoff events. Journal of Hydrology, 448, 39–59.

Cea, L., Bladé, E., 2015. A simple and efficient unstructured finite volume scheme for solving the shallow water equations in overland flow applications. Water Resources Research, 51 (7): 5464-5486.

Chow, V.T., 1959. Open channel hydraulics. McGraw-Hill Book Company, New York

Clark, C. O., 1945. Storage and the unit hydrograph. Transactions of the American Society of Civil Engineers, 110(1), 1419-1446.

Corradini, C, Melone, F, Singh, V., 1995. Some remarks on the use of GIUH in the hydrological practice. Nord. Hydrol. 297–312.

Costabile, P., Costanzo, C., Macchione, F., 2013. A storm event watershed model for surface runoff based on 2D fully dynamic wave equations. Hydrological Processes, 27(4), 554–569.

Costabile, P., Macchione, F., Natale, L., Petaccia, G., 2015. Flood mapping using LIDAR DEM. Limitations of the 1-D modeling highlighted by the 2-D approach. Natural Hazards, 77 (1), pp. 181-204.

Costabile, P., Costanzo, C., De Bartolo, S., Gangi, F., Macchione, F., Tomasicchio, G.R., 2019. Hydraulic characterization of river networks based on flow patterns simulated by 2-d shallow water modeling: scaling properties, multifractal interpretation and perspectives for channel heads detection. Water Resour. Res. 55, 7717–7752.

Costabile, P., Costanzo, C., De Lorenzo, G., Macchione, F., 2020. Is local flood hazard assessment in urban areas significantly influenced by the physical complexity of the hydrodynamic inundation model? Journal of Hydrology, 580, art. no. 124231, .

Costabile, P., Costanzo, C., 2021. A 2D-SWEs framework for efficient catchment-scale simulations: Hydrodynamic scaling properties of river networks and implications for non-uniform grids generation. J Hydrol, 599, 126306.

Costabile, P., Costanzo, C., De Lorenzo, G., De Santis, R., Penna, N., Macchione, F., 2021a. Terrestrial and airborne laser scanning and 2-D modelling for 3-D flood hazard maps in urban areas: new opportunities and perspectives Environmental Modelling and Software, 135, art. no. 104889.

Costabile, P., Costanzo, C., Ferraro, D., Barca, P., 2021b. Is HEC-RAS 2D accurate enough for storm-event hazard assessment? Lessons learnt from a benchmarking study based on rain-on-grid modelling. Journal of Hydrology, 603, art. no. 126962.

Costabile, P., Costanzo, C., Gandolfi, C., Gangi, F., Masseroni, D., 2022. Effects of DEM depression filling on river drainage patterns and surface runoff generated by 2D rain-on-grid scenarios. Water (under second review).

Delleur, R.A., Rao, R.A., 1974. Instantaneous unit hydrographs, peak discharges and time lags in urban basins. Hydrol. Sci. Bull. 19, 185–198.

Di Lazzaro, M., 2009. Regional analysis of storm hydrographs in the Rescaled Width Function framework. J. Hydrol. 373, 352–365.

Dullo, T.T., Gangrade, S., Morales-Hernández, M., Sharif, M.B., Kao, S.-C., Kalyanapu, A.J., Ghafoor, S., Evans, K.J., 2021. Simulation of Hurricane Harvey flood event through coupled hydrologic-hydraulic models: Challenges and next steps. Journal of Flood Risk Management, 14 (3), art. no. e12716, .

Ermini, R, Fiorentino, M., 1989. I tempi di ritardo caratteristici dei corsi d'acqua pugliesi, in Previsione e Prevenzione di Eventi Idrologici Estremi e Controllo- Rapporto 1989, Rossi F (Ed.), GNDCI National Research Council, Rome, 371-390 (in italian).

Fernández-Pato, J., Caviedes-Voullième, D., García-Navarro, P., 2016. Rainfall/runoff simulation with 2D full shallow water equations: Sensitivity analysis and calibration of infiltration parameters. Journal of Hydrology, 536, 496–513.

Fernández-Pato, J., Martínez-Aranda, S., García-Navarro, P., 2020. A 2D finite volume simulation tool to enable the assessment of combined hydrological and morphodynamical processes in mountain catchments. Advances in Water Resources, 141, art. no. 103617.

Ferraro, D., Costabile, P., Costanzo, C., Petaccia, G., Macchione, F., 2020. A spectral analysis approach for the a priori generation of computational grids in the 2-D hydrodynamic-based runoff simulations at a basin scale. Journal of Hydrology, 582, art. no. 124508.

Fieldman, A.D., 2000. Hydrologic Modeling System HEC-HMS Technical Reference Manuel. U.S. Army Corps of Engineers, Institute for Water Resources, Hydrologic Engineering Center (CEIWR-HEC), Davis, CA.

Folmar, N. D., Miller, A. C., 2008. Development of an empirical lag time equation. Journal of irrigation and drainage engineering, 134(4), 501-506.

Gericke, O.J., Smithers, J.C., 2014. Review of methods used to estimate catchment response time for the purpose of peak discharge estimation. Hydrol. Sci. J. 59, 1935–1971.

Gericke, O.J., 2019. GIS applications to investigate the linkage between geomorphological catchment characteristics and response time: A case study in four climatological regions, South Africa. Water (Switzerland), 11 (5), art. no. 1072.

Ghorbani, K., Salarijazi, M., Abdolhosseini, M., Eslamian, S., Ahmadianfar, I. 2019. Evaluation of Clark IUH in rainfall-runoff modelling (case study: Amameh Basin). International Journal of Hydrology Science and Technology, 9(2), 137 – 153.

Grimaldi, S., Petroselli, A., Tauro, F., Porfiri, M., 2012. Time of concentration: a paradox in modern hydrology. Hydrol. Sci. J. 57, 217–228.

Grimaldi, S., Petroselli, A., Nardi, F., 2012. A parsimonious geomorphological unit hydrograph for rainfall–runoff modelling in small ungauged basins. Hydrological Sciences Journal, 57, 73–83.

Haktanir, T., Sezen, N., 1990. Suitability of two-parameter gamma and three-parameter beta distributions as synthetic unit hydrographs in Anatolia. Hydrological Sciences Journal, 35 (2), 167–184.

Hickok, R. B., Keppel, R. V., Rafferty, B. R., 1959. Hydrograph synthesis for small arid land watersheds. Agricultural Engineering, 40(10), 608-611.

Kazezyılmaz-Alhana, C. M., Yalçına, İ., Javanshoura, K., Aytekinb, M., Gülbaza, S. 2020. A hydrological model for Ayamama watershed in Istanbul, Turkey, using HEC-HMS, Water Practice & Technology. 16(1), doi: 10.2166/wpt.2020.108.

Keifer, D.J., Chu, H.H. (1957). Synthetic Storm Pattern for Drainage Design. ASCE Journal of the Hydraulics Division, Vol. 83 (HY4), pp: 1332.1-1332.25.

Kirstetter, G., Hu, J., Delestre, O., Darboux, F., Lagrée, P.-Y., Popinet, S., Fullana, J.M., Josserand, C., 2016. Modeling rain-driven overland flow: Empirical versus analytical friction terms in the shallow water approximation. Journal of Hydrology, 536, pp. 1-9.

Kumar, R., Chatterjee, C., Singh, R. D., Lohani, A. K., Kumar, S., 2007. Runoff estimation for an ungauged catchment using geomorphological instantaneous unit hydrograph (GIUH) models. Hydrological Processes, 21(14), 1829–1840.

Lacasta, A., Morales-Hernández, M., Murillo, J., García-Navarro, P., 2015. GPU implementation of the 2d shallow water equations for the simulation of rainfall/runoff events. Environ. Earth Sci. 74 (11), 7295–7305.

Langbein, W.B., 1947.Topographic characteristics of drainage basins. U.S. Geol. Surv. Water-Supply Paper, 986 (C) , pp. 157-159.

Laouacheria, F., Mansouri, R., 2015. Comparison of WBNM and HEC-HMS for Runoff Hydrograph Prediction in a Small Urban Catchment. Water Resour. Manag. 29, 2485–2501.

Langridge, M., Gharabaghi, B., McBean, E., Bonakdari, H., Walton, R., 2020. Understanding the dynamic nature of Time-to-Peak in UK streams. Journal of Hydrology, 583, art. no. 124630.

Leopold, L.B., 1991. Lag times for small drainage basins. Catena 18, 157–171.

Loukas, A., Quick, M.C., 1996. Estimation physique du temps de réponse de bassins forestiers de montagne. Hydrol. Sci. J. 41, 1–19.

McEnroe, B.M., Zhao, H., 2001. Lag times of urban and developing watersheds in Johnson County, Kansas. Kansas. (available at: https://ntlrepository.blob.core.windows.net/lib/18000/18700/18705/PB2002101487.pdf).

Melone, F., Corradini, C., Singh, V.P., 2002. Lag prediction in ungauged basins: An investigation through actual data of the upper tiber river valley. Hydrol. Process. 16, 1085–1094.

Meyersohn, W.D., 2016. Runoff Prediction for Dam Safety Evaluations Based on Variable Time of Concentration. J. Hydrol. Eng. 21, 04016031.

Michailidi, E.M., Antoniadi, S., Koukouvinos, A., Bacchi, B., Efstratiadis, A., 2018. Timing the time of concentration: shedding light on a paradox. Hydrol. Sci. J. 63, 721–740.

Mimikou, M., 1984. Regional relationships between basin size and runoff characteristics. Hydrol. Sci. J. 29, 63–73.

Ming, X., Liang, Q., Xia, X., Li, D., Fowler, H.J., 2020. Real-Time Flood Forecasting Based on a High-Performance 2-D Hydrodynamic Model and Numerical Weather Predictions. Water Resources Research, 56 (7), art. no. e2019WR025583.

Mitchell, W. D., 1948. Unit hydrographs in Illinois. Illinois Department of Public Works and Buildings, Division of Waterways.

Morales-Hernández, M., Sharif, M.B., Kalyanapu, A., Ghafoor, S.K., Dullo, T.T., Gangrade, S., Kao, S.-C., Norman, M.R., Evans, K.J., 2021. TRITON: A Multi-GPU open source 2D hydrodynamic flood model. Environmental Modelling and Software, 141, art. no. 105034, .

Nash, J. E. 1957. The form of the instantaneous unit hydrograph. International Association of Hydrological Sciences, 45, 114–121.

Nash, J., 1960. A unit hydrograph study, with particular reference to British catchments. Proc. Inst. Civ. Eng. 249–282.

Nash, J. E., Sutcliffe, J. V. 1970. River flow forecasting through conceptual models part I- A discussion of principles. Journal of Hydrology. 10 (3): 282–290.

Natural Environmental Research Council (NERC), 1975. Flood studies report. London.

Natural Resources Conservation Service (NRCS). 2010. Chapter 15: Time of concentration. In National engineering handbook, Part 630, Hydrology. Washington, DC: Author

Ni, Y., Cao, Z., Liu, Q., Liu, Q., 2020.A 2D hydrodynamic model for shallow water flows with significant infiltration losses. Hydrological Processes, 34 (10), pp. 2263-2280.

Padulano, R., Costabile, P., Costanzo, C., Rianna, G., Del Giudice, G., Mercogliano, P. (2021). Using the present to estimate the future: A simplified approach for the quantification of climate change effects on urban flooding by scenario analysis. Hydrological Processes, 35 (12), art. no. e14436, .

Pavlovic, S.B., Moglen, G.E., 2008. Discretization Issues in Travel Time Calculation. J. Hydrol. Eng. 13, 71–79.

Pechlivanidis, I.G., McIntyre, N., Wheater, H.S., 2017. The significan ce of spatial variability of rainfall onsimulated runoff: An evaluation based on the Upper Lee catchment, UK Hydrology Research, 48 (4), pp. 1118-1130.

Ponce, V.M., Hawkins, R.H., 1996. Runoff curve number: Has it reached maturity?. Journal of Hydrologic Engineering, 1 (1), pp. 11-18.

Putnam, A., 1972. Rainfall and runoff in urban areas: a case study of flooding in the Piedmont of North Carolina, in: Proceedings of the Urban Rainfall Management Problems Conference. University of Kentucky, Lexington.

Ravazzani, G., Boscarello, L., Cislaghi, A., Mancini, M., 2019. Review of Time-of-Concentration Equations and a New Proposal in Italy. Journal of Hydrologic Engineering, 24 (10), art. no. 04019039.

Rigon, R., Bancheri, M., Formetta, G., de Lavenne, A. 2016. The geo-morphological unit hydrograph from a historical-critical perspective. Earth Surface Processes and Landforms, 41(1), 27–37.

Rodriguez-Iturbe, I., Valdés, J. B., 1979. The geomorphologic structure of hydrologic response. Water Resources Research, 15(6), 1409–1420.

Rossi, F., 1974. Criteri di similitudine idrologica per le stime della portata al colmo di piena corrispondente ad un assegnato tempo di ritorno, in: Naples, U. of (Ed.), Atti XXV Convegno Di Idraulica e Costruzioni Idrauliche. Naples, pp. 235–261. (in Italian),

Selvalingam, S., Liong, S.Y., Manoharan, P.C., 1987. Use of RORB and SWMM models to an urban catchment in Singapore. Adv. Water Resour. 10, 78–86.

Shi, W., Wang, N., Wang, M., Li, D., 2021. Revised runoff curve number for runoff prediction in the Loess Plateau of China. Hydrological Processes, 35 (10), art. no. e14390, .

Simas, M.J.C. and Hawkins, R.H., 2002. Lag time characteristics in small watersheds in the United States. In: Proceedings of the 2nd federal interagency hydrologic modelling conference. Las Vegas, Nevada: FIHMC, 1–7.

Snyder, F.F., 1938. Synthetic unit hydrographs. Transactions, American Geophysical Union, 19, 447.

Taccone, F., Antoine, G., Delestre, O., Goutal, N., 2020. A new criterion for the evaluation of the velocity field for rainfall-runoff modelling using a shallow-water model. Advances in Water Resources, 140, art. no. 103581.

Talei, A., Chua, L.H.C., 2012. Influence of lag time on event-based rainfall-runoff modeling using the data driven approach. J. Hydrol. 438–439, 223–233.

Tügel, F., Hassan, A., Hou, J., Hinkelmann, R., 2021. Applicability of Literature Values for Green–Ampt Parameters to Account for Infiltration in Hydrodynamic Rainfall–Runoff Simulations in Ungauged Basins. Environmental Modeling and Assessment. 10.1007/s10666-021-09788-0.

Watt, W.E., Chow, K.C.A., 1985. A general expression for basin lag time. Can. J. Civ. Eng. 12, 294–300.

Wu, S.J., Yeh, K.C., Ho, C.H., Yang, S.H., 2016. Modeling probabilistic lag time equation in a watershed based on uncertainties in rainfall, hydraulic and geographical factors. Hydrol. Res. 47, 1116–1141.

Xia, X., Liang, Q., Ming, X., Hou, J. 2017. An efficient and stable hydrodynamic model with novel source term discretization schemes for overland flow and flood simulations. Water Resources Research, 53, 3730–3759.

Yu, B., Rose, C.W., Ciesiolka, C.C.A., Cakurs, U., 2000. The relationship between runoff rate and lag time and the effects of surface treatments at the plot scale. Hydrol. Sci. J. 45, 709–726.

Yu, C., Duan, J., 2017. Simulation of surface runoff using hydrodynamic model. Journal of Hydrologic Engineering, 22 (6), art. no. 04017006.

Zhang, S., Liu, C., Yao, Z., Guo, L., 2007. Experimental study on lag time for a small watershed. Hydrological Processes, 21 (8), pp. 1045-1054.

Zeng, Q., Chen, H., Xu, C.-Y., Jie, M.-X., Chen, J., Guo, S.-L., Liu, J., 2018. The effect of rain gauge density and distribution on runoff simulation using a lumped hydrological modelling approach. Journal of Hydrology, 563, pp. 106-122.

Zuazo, V., Gironás, J., Niemann, J.D., 2014. Assessing the impact of travel time formulations on the performance of spatially distributed travel time methods applied to hillslopes. Journal of Hydrology, 519 (PB), pp. 1315-1327.

HIGHLIGHTS

- Use of 2D-SWEs model to provide evidence on the variability of the lag time in small basins
- Lag time estimation on the basis of characteristic times influencing the hydrodynamic response
- Satisfying results in relation to the observed lag times
- Competitive predictions in respect to literature formulas

LIST OF FIGURES

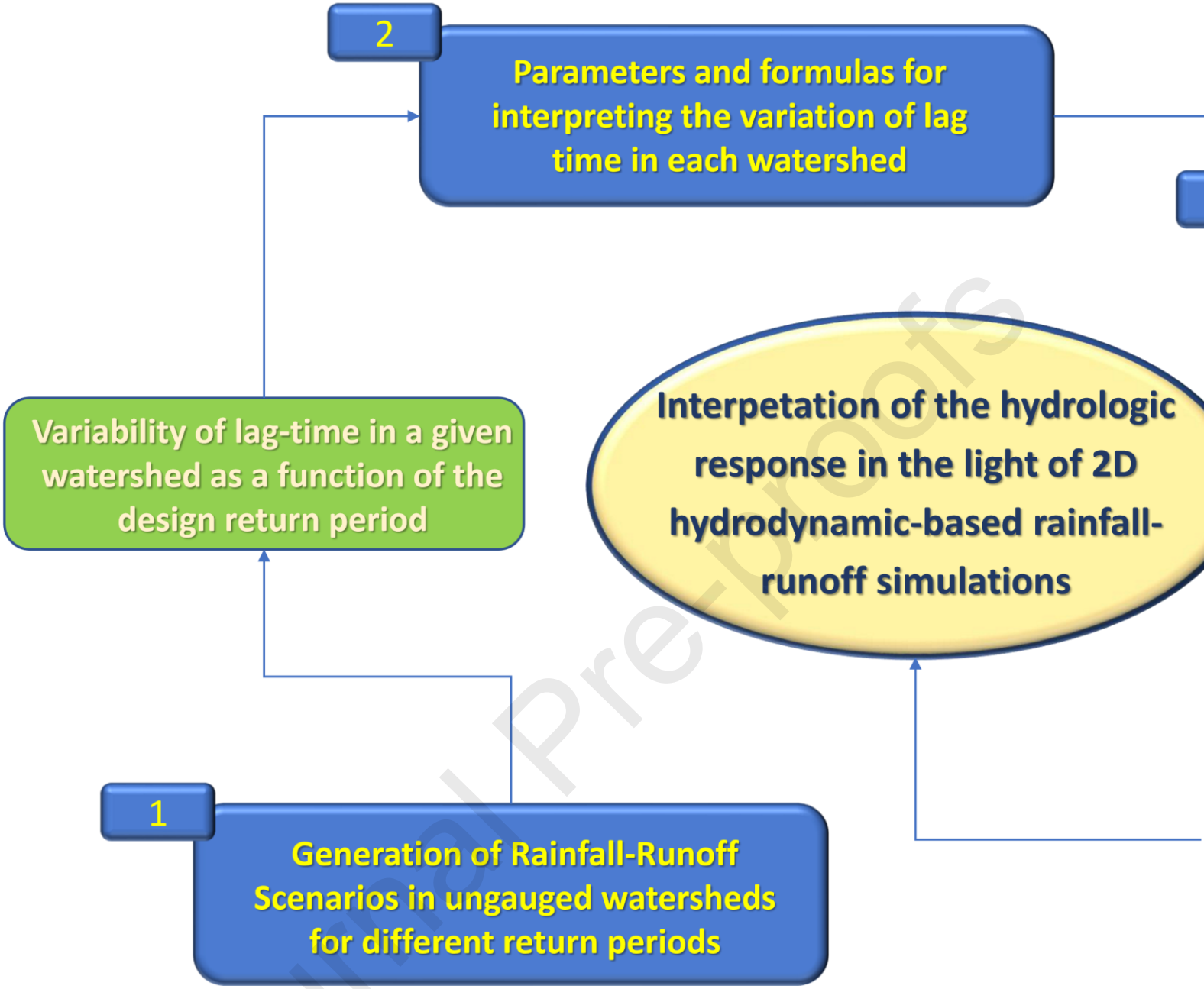

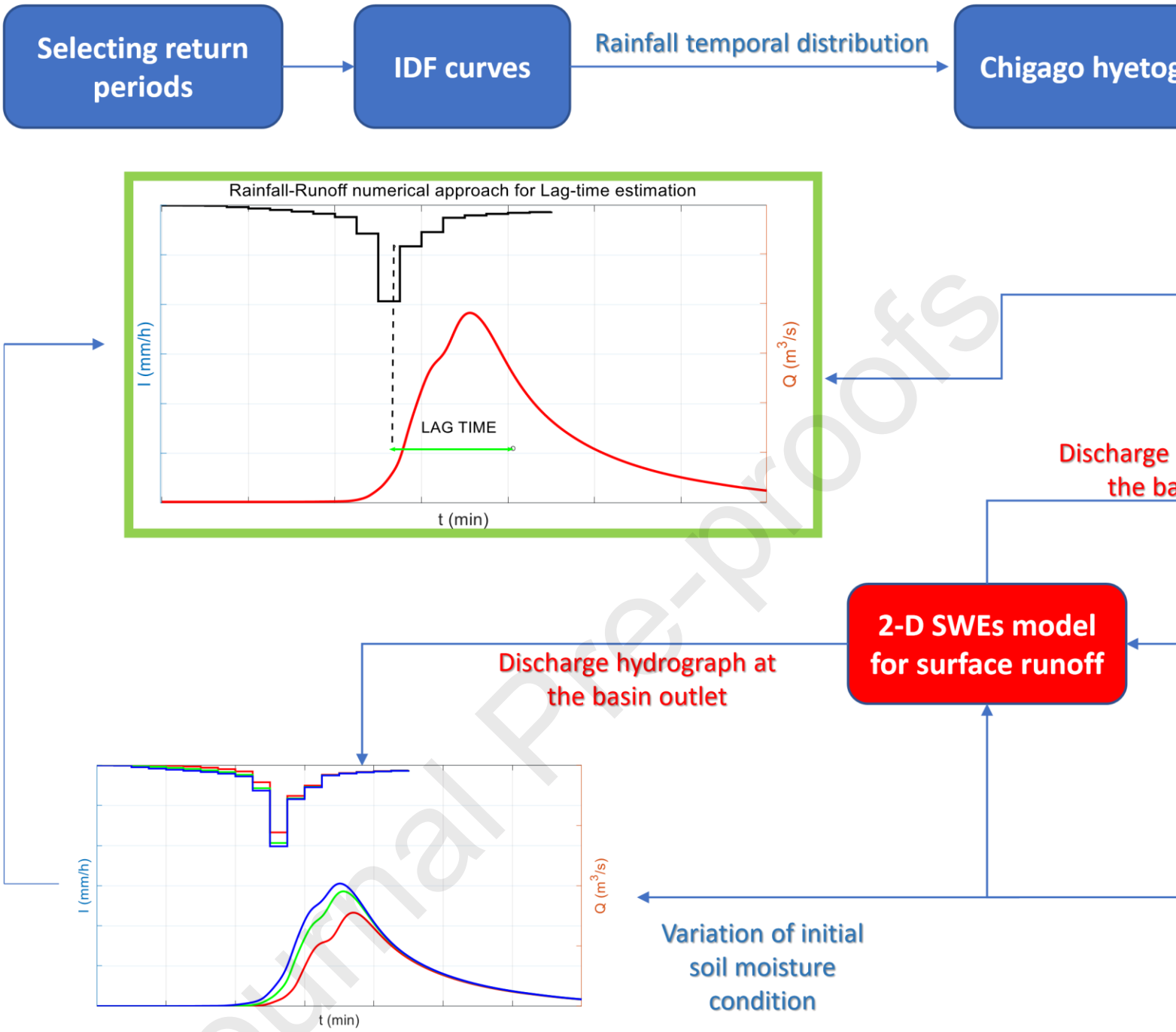

ARDIVESTRA - CORINE LAND COVER MAP/ROUGHNESS MAP

(a)

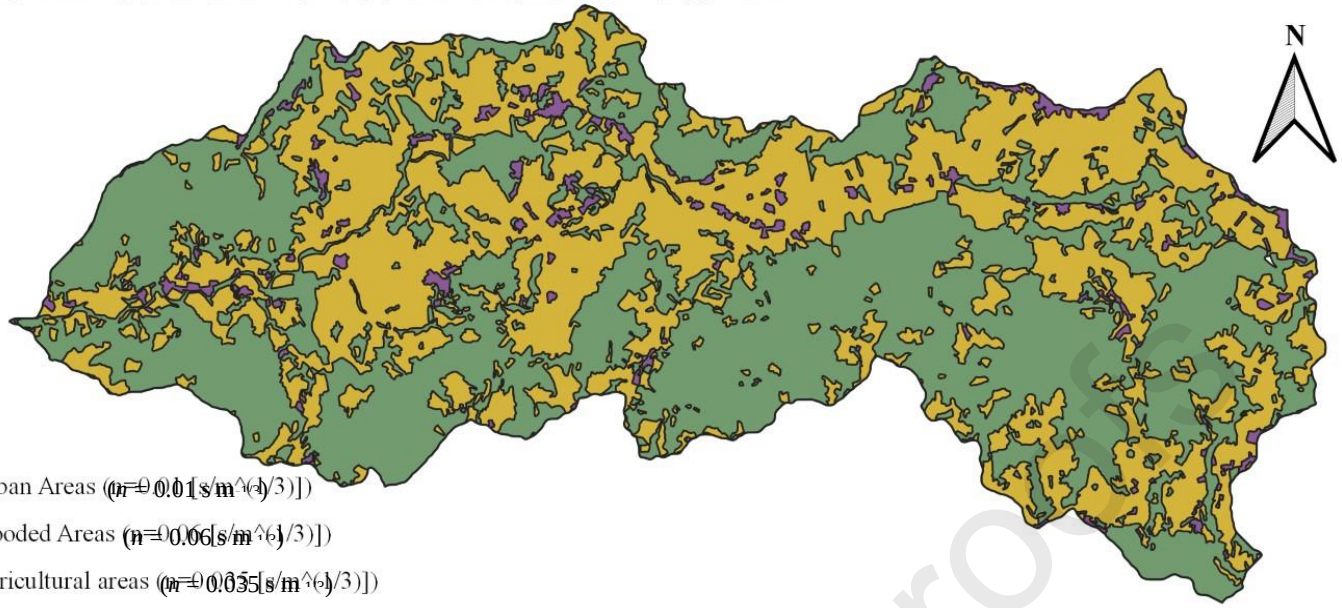

ARDIVESTRA - GEOLOGICAL MAP

(b)

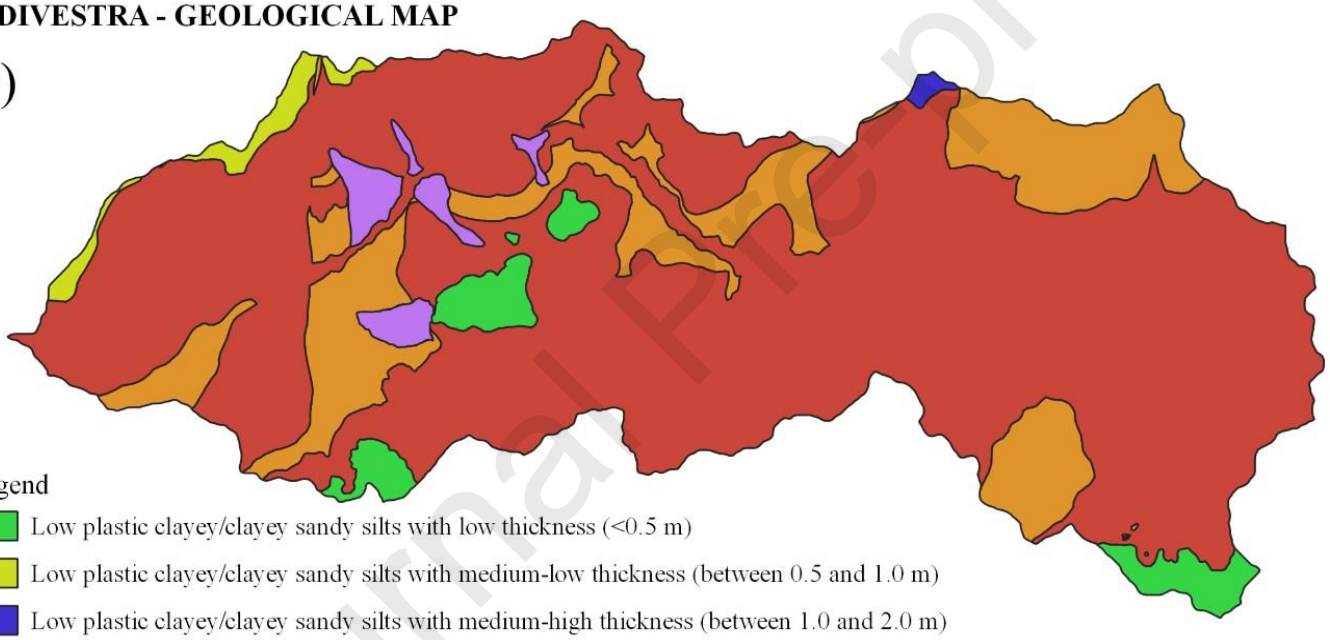

ARDIVESTRA - CN MAP

(c)